Chemical Characteristics And Factors Affecting Groundwater Chemistry From The Yellow River Irrigation Area In Tumochuan Plain In The Middle And Upper Reaches of The Yellow River Basin

Zihe Wang (wangzihe_168@163.com)
IWHR: China Institute of Water Resources and Hydropower Research https://orcid.org/0000-0003-0460-9596
Jing Jin
IWHR: China Institute of Water Resources and Hydropower Research
Wei Liu
IWHR: China Institute of Water Resources and Hydropower Research
Tenglin Deng
IWHR: China Institute of Water Resources and Hydropower Research
Yiping Zhao
IWHR: China Institute of Water Resources and Hydropower Research
Xiaofeng Du
IWHR: China Institute of Water Resources and Hydropower Research

Research Article

Keywords: Middle and upper reaches of the Yellow River Basin, the Yellow River irrigation area, Characteristics of hydrogen and oxygen isotopes, Chemical characteristics of groundwater

Posted Date: September 9th, 2021

DOI: https://doi.org/10.21203/rs.3.rs-584081/v1

Abstract

The Yellow River irrigation area in Tumochuan Plain is one of the primary grain production areas in the middle and upper reaches of the Yellow River Basin (YRB). The groundwater in the area is bitter and salty, which significantly influences drinking water safety of residents. To investigate its chemical characteristics and material sources, we collected 12 groundwater samplings, 3 irrigation water samplings, and 1 precipitation sample during the winter irrigation period (WIP) in November 2016 and the spring irrigation period (SIP) in April 2017, respectively. We then analysed the hydrogen and oxygen stable isotopes and hydrochemical characteristics of the shallow groundwater in the study area and investigated their affecting factors by using environmental isotopes, Gibbs diagrams, Schoeller diagrams, and ion proportionality coefficient analysis. Next, we qualitatively analysed the material sources. The results show the followings: (1) The concentrations of major ions in groundwater in the SIP are generally higher than in the WIP, which may be recharged by snow melting water in the spring. (2) The average values of δD and $\delta^{18}O$ for the groundwater are -78.0‰ and -10.3‰, respectively, in the WIP and -77.4‰ and -10.3‰, respectively, in the SIP. However, the characteristics of hydrogen and oxygen isotopes in the groundwater are almost identical in the WIP and SIP. (3) The formation of groundwater chemical constituent are controlled by evaporation concentration and lixiviation, and dissolution of evaporite and mirabilite is the most important factor. Synchronously, the formation of groundwater chemical constituent is also influenced ion exchange and human activities. The study provides effective guidance for groundwater resource development in arid and semi-arid regions.

Introduction

Hetao Plain, including the Qiantao Plain (Tumochuan Plain) and the Houtao Plain (Bayannur Plain), covers approximately 21,000 km^2 in total (Liu et al. 2017). The Tumochuan Plain features Hohhot, the capital city of Inner Mongolia, and Baotou, an important industrial city. It is the political, economic, and cultural centre of Inner Mongolia. Agricultural production in the Yellow River irrigation area of Tumochuan Plain, one of irrigation areas in northwestern China, depends highly on irrigation. Due to unreasonable irrigation method, the soil salinization and secondary salinization phenomenon has become increasingly serious. As a result, a large amount of land has been abandoned, and the single source of drinking water continues to deteriorate, endangering the drinking water safety of the local population.

Conventional methods of hydrochemical analysis include histogram analysis, Piper diagrams (Piper 1944; He and Li 2020), Gibbs diagrams (Gibbs 1970) and ionic ratios (Han et al. 2013; Farid et al. 2015; Li et al. 2016a, b). Although these approaches are often simple and intuitionistic, they are restricted by the limited number of chemical variables of groundwater. Among these methods, combining the analysis of hydrogen and oxygen isotopes with hydrochemistry to investigate sources of groundwater recharge at the watershed scale has attracted great attention from scholars worldwide (Anne and Kirsti 2015; Guo et al. 2015; Qian et al. 2013, 2014;). For example, Li et al. (2016c) integrated stable hydrogen and oxygen isotopes and hydrochemistry and proposed a method to quantify the connectivity between river water and groundwater. Their research can be of great value for comprehensive understanding of surface water and groundwater interaction. Scanlon et al. (2006) studied the characteristics and patterns of groundwater recharge in arid and semi-arid regions using stable hydrogen and oxygen isotopes. Wang et al. (2013) applied hydrogen and oxygen isotopes and hydrochemistry to analyse the sources of groundwater recharge in Hetao Plain in Inner Mongolia. Adhikary et al. (2014) utilized hydrogen and oxygen stable isotopes and hydrochemistry to investigate the composition and possible sources of groundwater pollutants in New Delhi and determined the boundary between anthropogenic and natural pollution and the capability for renewal of groundwater by examining variation in chloride ion concentration. Li et al. (2019b) explored the hydrochemical evolution of groundwater and its controlling factors in Yinchuan by utilizing hydrochemical and isotope characteristics. Zhao et al. (2019) applied hydrochemical and isotope characteristics to analyse the spatiotemporal evolution of groundwater in the Hangzhou Bay New Zone and evaluated its mechanism of formation and renewal capability. Therefore, combining analysis of hydrogen and oxygen stable isotopes with hydrochemistry holds significant potential for elucidating water-rock interactions and protecting groundwater.

However, most studies of groundwater have been conducted on the Bayannur Plain (He et al. 2010; Guo et al. 2010; Guo et al. 2012; Wang et al. 2013; Gao et al. 2014). Few studies of groundwater have been conducted on the Tumochuan Plain, which is especially true for investigations of hydrochemical characteristics, sources and controlling factors of groundwater (Feng et al. 2016; Wang et al. 2017b). Therefore, the principle objective of this study are to (1) delineate the hydrochemical characteristics and factors affecting of groundwater in the Yellow River irrigation area of the Tumochuan Plain, the upper and middle reaches of YRB, and (2) identify environmental isotope characteristics and the origin of the groundwater. As introduced by Li (2020a, b), the ecological protection and high-quality development in YRB has become a major strategy for national development. This study will provide a basis for promoting sustainable development and utilization of groundwater resources in YRB, and provide a useful guidance for improving local safe water supply and is also applicable in similar situations.

Study Area

Location and Climate

The study area is located along the northern of Yellow River with a total area of 1275 km^2 in the Tumd Right Banner of Baotou City, Inner Mongolia Autonomous Region, China (Fig.1). The study area is bounded between latitude 40°10´-40°51´N and longitude 110°15´-111°12´E, and belongs to the warm temperate arid and semi-arid climate zone. The rainfall in the area is concentrated in July to September with the average annual of rainfall of about 356.6 mm. The long-term average potential evaporation is approximately 1989.6mm and the annual average is 6.9 ℃.

Geological and hydrogeological settings

Since the Pleistocene, the study area, continuously sinking, has always been deposited with thick silty sediments, mostly lacustrine sediments. The central lacustrine facies dominated by the upper section of the middle Pleistocene series (Q_2) is distributed over the Maodai-Mingshanao-Yellow River, buried more than 89.39 meters underground. The lithology is characterised by grey, sage green-ash black silty sand, sandy clay, or clay and silt interbeds, mingled with mirabilite beds. Mirabilite beds extend to the south of Minshengqu and north of Ershisiqingdi-Shahaizi and reach Shandai and Dadai of Tumd Left Banner in the east and Dalad Banner in the west, which is about 70 km long and 11km wide, with depth between 120 and 170 m. At the present time, 1-4 layers can be seen within the depths revealed, with a total thickness of 9.84 m and a stable horizontal distribution. Analysis of water-soluble salts shows 32.01-51.79 g mirabilite per 100 g water, and the total water-soluble salts contain 94.97-99.58% of pure mirabilite (Na_2SO_4). The upper section of central lacustrine facies, with alternating deposits of piedmont alluvium and diluvium, exhibits a lithology of clay and sandy clay intercalated with silty sand beds.

The aquifers in the study area are phreatic-feeble confined aquifers and are mainly composed of medium-fine sand and silty fine sand. There are generally 2 water-resisting layers in the central area, and each single layer is thick, with the highest thickness being approximately 40 m. In other areas, there are normally 4 water-resisting layers of cohesive soil, each layer with a thickness ranging from 5 m to 20 m. Around the Yellow River, the number of water-resisting layers tends to be more, while the thickness of a single layer is thin. In general, thickness of aquifers ranges from 80 m to 100 m in the northwest, from 40 m to 80 m in the central area, and from 20 m to 40 m in the east in the study area. From the piedmont plain to the bank of the Yellow River, the lithology of aquifers changes from medium-fine sand to fine sand and silty fine sand. In the areas around the Yellow River, the aquifer is mainly composed of fine sand and silty fine sand. The depth of the groundwater level ranges from 5 to 10 m near the piedmont and from 2 to 5 m near the Yellow River (Fig. 2).

The groundwater in the study area is mainly recharged by lateral groundwater of the piedmont plain of Daqing Mountain, irrigation infiltration, and rainfall infiltration. Along the northwest-southeast direction, the runoff flows from leading edge of the piedmont plain to the Hasu Lake and the Yellow River. In particular, Hasu Lake, Shandai Village, Dadai Village and Shahaizi Village constitute areas where shallow groundwater converges.

Materials and methods

During the WIP in November 2016 and the SIP in April 2017, we investigated the Yellow River irrigation area on the Tumochuan Plain. Sixteen representative groundwater (n=12) and irrigation water (n=3) and precipitation (n=1) samples were selected in November 2016, and the same sampling points and numbers were selected in April 2017.The locations of sampling sites are shown in Fig. 1. We measured temperature, pH value, conductivity, and content of dissolved oxygen of groundwater and irrigation water with a portable HACH multi-parameter water quality meter in the field. After filtering with a GF/F filter in the field, some samples used for major ion analysis were kept in 1,000-ml plastic bottles and sealed with parafilm sealing film, and others used for the stable isotope (D, ^{18}O) analysis were put in 100-ml glass bottles and sealed with parafilm sealing film. The concentrations of K^+, Na^+, Ca^{2+} and Mg^{2+} were measured through inductively coupled plasma in the laboratory, and the concentrations of SO_4^{2-}, Cl^-, and HCO_3^- were analyzed with ion chromatography. Stable isotope of D and ^{18}O were determined with a MAT-253 gas isotope ratio mass spectrometer. After measuring each sample six times, the mean value was taken. The precision for the stable isotope (D, ^{18}O) measurements were ±1.0‰ and ±0.1‰, respectively.

Results And Analysis

General hydrochemistry

The statistical summary of the results of hydrochemical parameters of the groundwater in the study area are listed in Table 1. The pH was found to range from 7.88 to 8.40 with a mean of 8.18, and the mean TDS of the groundwater was 7,625.81 mg/L. Overall, the pattern for the mean anions and cations concentrations was, in decreasing order, $SO_4^{2-}>Cl^->HCO_3^->NO_3^-$ and $Na^+>Mg^{2+}>Ca^{2+}>K^+$, respectively. The average contents of Na^+, SO_4^{2-} and Cl^- are much higher than other ions in groundwater, regardless of reason. In the WIP, the concentration of K^+ ranges from 3.36 to 25.38 mg/L with a mean of 11.16 mg/L, and the concentration of Na^+ ranges from 153.20 to 6,087 mg/L with a mean of

2,353.10 mg/L, and the concentration of Ca^{2+} ranges from 16.90 to 433.08 mg/L with a mean of 132.36 mg/L, and the concentration of Mg^{2+} ranges from 30.08 to 923.20 mg/L with a mean of 282.47 mg/L. The concentrations of main ions of groundwater in the WIP are a little higher than in the SIP, which may be melt snow and ice in spring.

Table 1
Statistical results of hydrochemical parameters of groundwater

Sampling time	Item	K^+	Na^+	Ca^{2+}	Mg^{2+}	Cl^-	HCO_3^-	SO_4^{2-}	NO_3^-	TDS	pH
WIP in November 2016	Average	11.16	2353.10	132.36	282.47	2051.82	991.98	2885.43	6.13	8741.77	8.18
	Median	8.10	2288.00	119.70	134.85	1777.00	844.50	996.65	5.11	7755.47	8.21
	Standard deviation	7.60	2026.31	101.40	269.32	2061.47	634.02	3116.46	5.35	7000.00	0.18
	Min	3.36	153.20	16.90	30.08	146.20	311.20	1.68	1.47	1116.10	7.88
	Max	25.38	6087.00	433.80	923.20	7730.00	2219.00	8154.00	22.5	20784.26	8.40
SIP in April 2017	Average	11.89	1746.63	112.11	247.15	1740.08	691.43	1936.81	10.09	6509.86	8.21
	Median	7.73	1637.50	80.79	124.94	1529.00	571.85	967.35	7.92	5795.40	8.23
	Standard deviation	8.93	1422.11	103.90	256.00	1939.05	382.23	1964.11	7.80	4961.54	0.17
	Min	3.53	110.60	16.26	28.52	120.50	302.60	4.59	3.66	903.02	7.95
	Max	28.05	3843.00	437.90	949.50	7587.00	1398.00	5146.00	34.44	14211.64	8.43

Among all the samples, the concentrations of SO_4^{2-} of the groundwater sampled in the sites of Tianjiagedan Village, Wujuniu Village, Lianhe Village, Jinqianpu Village, Saiwusu Village, and Dongheishatu Village ranges from 1,083 to 8,154 mg/L with the mean of 5,442.5 mg/L, and others are less than 1,000 mg/L. It may be the sampling sites are within the mirabilite zone, and the site in Jinqianpu Village is close to the centre of the mirabilite zone. Other sampling sites are far from the mirabilite zone, so the concentration of SO_4^{2-} is relatively low (Table 1、2).

Hydrochemical facies of groundwater

The Piper diagram is composed of two ternary diagrams showing anions and cations and a diamond plot reflecting the hydrochemical characteristics (Piper 1944; Huang et al. 2019; He and Li 2020). It can clearly show hydrochemical characteristics and types of water samples, without being influenced by human factors. We are able to clearly distinguish the groundwater, irrigation water and precipitation in the study area with the Piper diagram constructed, with precipitation indicated on the left and groundwater on the right. Hydrochemical types and distributions of the groundwater regardless of reason were almost identical (Fig. 3). There are four hydrochemical types of groundwater, i.e., HCO_3•Cl•SO_4-Na•Ca•Mg, SO_4•Cl-Na, HCO_3•Cl-Na•Mg, and Cl-Na. From northwest to southeast, the hydrochemical type changed from HCO_3•Cl•SO_4-Na•Ca•Mg to SO_4•Cl-Na and finally to Cl-Na. The central area contained a high concentration of SO_4^{2-}, which may be attributed to dissolution of mirabilite. The irrigation water in the WIP was mainly the Cl•SO_4•HCO_3-Na•Mg•Ca type, and that during the SIP was Cl•HCO_3-Na•Ca type. The irrigation water samples selected during two periods comes from the Yellow River, whose components are determined by the river water.

Process that influence hydrogeochemistry of groundwater

Primary contronlling factors of hydrochemical evolution

The Gibbs diagram is often used to analyse how rock-water interaction influences the mechanism of hydrogeochemistry evolution (Ren et al. 2021; Wu et al. 2020; He et al. 2019). By utilizing the relationships among total dissolved solids (TDS), Na^+, Ca^{2+}, Cl^-, and HCO_3^- in rivers, lakes and major oceans across the world, Gibbs classified the affecting factors of hydrochemical components of natural water into precipitation dominance, rock-water interaction dominance, and evaporation dominance (Gibbs 1970). In recent years, many scholars have studied how water-rock interaction influences hydrogeochemical processes by using Gibbs diagrams (Wang et al. 2014;Sun et al. 2018;Chen et al. 2019; He and Wu 2019; Li et al. 2019a; Zhang et al. 2018). Groundwater is greatly affected by rock-water interaction, which forms the zone a little bigger than surface water forms in the Gibbs diagram (Marandi and Shand 2018). In the Gibbs diagram, the water samples with low TDS vs high equivalence ratio of $Na^+/(Na^+{+}Ca^{2+})$ plot in the precipitation dominance zone, i.e., lower right of the diagram, which indicates that the main ion contents in water body are affected by meteoric water; and the water samples with medium TDS vs low equivalence ratio of $Na^+/(Na^+{+}Ca^{2+})$ plot in the rock-water interaction dominance zone, i.e., middle left of the diagram, which implies that the main ion contents in water body are affected by rock-water interaction; and the water samples with high TDS and vs high equivalence ratio of $Na^+/(Na^+{+}Ca^{2+})$ plot

in the evaporation dominance zone, i.e., upper right of the diagram, which signifies that water samples mostly come from arid and semi-arid areas (Xiao et al. 2012; Zhang et al. 2017).

According to the Gibbs diagram for groundwater in the study area, the equivalence ratio of Na^+/ (Na^++Ca^{2+}) ranges from 0.63 to 0.99 with an average of 0.84, and all values exceeded 0.5(Fig. 4a). At the same time, the equivalence ratio of Cl^-/ (Cl^-+HCO_3^-) ranges from 0.23 to 0.90 with an average of 0.55, and approximately half of the values exceeded 0.5(Fig. 4b). The Gibbs diagram indicates that the water samples, regardless of season, shows the same pattern of distribution. The irrigation water samples plot in rock-water interaction zone, and the groundwater samples plot in the rock-water interaction zone and evaporation dominance zone of the Gibbs diagram, with evaporation playing the dominant role, which suggests that the main iron contents in groundwater are affected by mineral dissolution besides of evaporation. Some groundwater samples plot outside the zone, which indicates that the iron contents in the groundwater may be affected by human activities.

Ionic relations and sources of major components of groundwater

With rock-weathering and water-rock interaction, the minerals of rocks dissolve in the water, which can affect hydrochemical components. (Zhang et al. 2018; Wang et al. 2017a).

The molar ratio of (Na^++K^+)/(Cl^-) of almost all samples regardless of season in the study area plot above the line with a slope of 1 (Fig. 5a), which indicates that in addition to dissolution of rock-salt, hydrochemical components of the groundwater may also be influenced by dissolution of sodium salt. Meanwhile, samples in throughflow area plot far from the line with a slope of 1, which implies cation exchange plays significant role in affecting hydrochemical contents.

The molar ratio of (Ca^{2+}+Mg^{2+})/(HCO_3^-) of almost all samples regardless of season in the study area plot above the line with a slope of 1 (Fig. 5b), which indicates in addition to dissolution of calcite and dolomite, hydrochemical components of the groundwater may also be influenced by dissolution of minerals that contain Ca^{2+}.

The molar ratio of (Ca^{2+}+Mg^{2+}) /(HCO_3^- + SO_4^{2-}) of almost all samples regardless of season in the study area plot below the line with a slope of 1 (Fig. 5c), which implies that a part of contents of Ca^{2+} in the groundwater derives from the dissolved evaporite (gypsum)(Ma et al. 2018; Redwan and Abde 2016).

The molar ratio of (SO_4^{2-}+Cl-)/ (HCO_3^-) of almost all samples regardless of season in the study area plot above the line with a slope of 1 (Fig. 5d), which signifies that major ions in the groundwater are provided by the dissolved evaporate and the dissolved gypsum may be the source of the Ca^{2+}.

The molar ratio of Ca^{2+}/ SO_4^{2-} of almost all samples regardless of season in the study area plot under the line with a slope of 1 (Fig. 5e), which testifies the dissolved gypsum is main source of the Ca^{2+}. Furthermore, the concentrations of Na^+ and SO_4^{2-} in groundwater is high, which deduces that the source of Na^+ and SO_4^{2-} may be mainly derived from the dissolved albite and mirabilite

The molar ratio of (Ca^{2+}+Mg^{2+}-HCO_3^-)/ [(SO_4^{2-}-(Na^+-Cl^-)] of almost all samples regardless of season in the study area plot near the line with a slope of 1 (Fig. 5f), which further demonstrates that the dissolved gypsum and mirabilite are the main source of the SO_4^{2-}.

Ion exchange

In the long process of interactions between groundwater and rock, cation exchange may occur (Shen 1993; Wu et al. 2014). Cation exchange is generally identified according to the bivariate diagram of (Ca^{2+}+Mg^{2+}-SO_4^{2-}-HCO_3^-) versus (Na^++K^+-Cl^-). When cation exchange occurs, the ratio between (Ca^{2+}+Mg^{2+}-SO_4^{2-}-HCO_3^-) and (Na^++K^+-Cl^-) should be approximately − 1 (Xiao 2015). As shown in Fig. 6(a), most water samples, regardless of season, plot near the line with a slope of -1, which indicates that cation exchange is taking place in the aquifers and plays an important role in the evolution of water chemistry in the study area. The ion exchange equation is defined as formulae 1.

$Na_2X + Ca^{2+} \rightleftarrows Na^+ + CaX$ (1)

In addition, the chloro-alkaline indices (CAI-1 and CAI-2) were used to explore the occurrence of cation exchange in groundwater, which are expressed as follows formulae 2 and 3, where the unit of all ions is meq/L (Schoeller 1977; Li et al. 2018; Wu et al. 2015; Su et al. 2020).

$$\mathrm{CAI}-1=\frac{\mathrm{Cl}^{-}-\left(\mathrm{Na}^{+}+\mathrm{K}^{+}\right)}{\mathrm{Cl}^{-}} \quad (2)$$

$$CAI-2=\frac{Cl^{-}-(Na^{+}+K^{+})}{SO_4{}^{2-}+HCO_3{}^{-}+CO_3{}^{2-}+NO_3{}^{-}} \quad (3)$$

As shown in the Fig. 6(b), almost water samples regardless of season plot in the lower left region, where CAI-1 and CAI-2 values are less than zero, which indicates that cation exchanges occur widely in the study area and that Ca^{2+} is absorbed while Na^{+} is released in water, increasing the concentration of Na^{+} and decreasing the concentration of Ca^{2+}. Cation exchange is likely a vital source of Na^{+} in groundwater and irrigation water.

Characteristics of hydrogen and oxygen isotopes

The stable isotopes (δD and $\delta^{18}O$) are often used to indicate the recharge sources and evolution of groundwater (Gui and Chen 2016; Qian et al. 2013, 2014). By comparing the curve of the relationship of δD and $^{\delta 18}O$ with the meteoric water line, we can determine how groundwater is formed and migrates (Huang et al. 2019; Qi et al. 2019). In 1967, the global meteoric water line (GMWL) was established by Craig according to the relationship between δD and $\delta^{18}O$, i.e., $\delta D = 8\delta^{18}O+10$ (Craig 1961). The GMWL provides a benchmark for the composition of isotopes in meteoric water and a reference for deducing the sources of groundwater. The local meteoric water line (LMWL) of Baotou is expressed as $\delta D = 6.36\delta^{18}O-5.21$, which was established by Wang et al. (2013) and may be deemed as components of hydrogen and oxygen isotopes in modern precipitation in the study area. And the average values of $\delta^{18}O$ and δD in LMWL are − 8.16‰ and − 57.10‰, respectively, which come from the Global Network of Isotopes Precipitation database.

The stable isotopes (δD and $\delta^{18}O$) of the groundwater samples selected in the WIP were found to range from − 87‰ to -67‰ with an average of -78.0‰ and from − 11.5‰ to -8.5‰ with an average of -10.3‰, respectively; and of irrigation water are found to -64‰ and − 8.8‰, respectively; and of precipitation are found to -75‰ and − 11.0‰, respectively (Table 2). Meanwhile, the stable isotopes (δD and $\delta^{18}O$) of the groundwater samples selected in the SIP were approximately the same as the values of samples measured in the WIP.

Table 2

Analytical results of δD and $\delta^{18}O$ of groundwater irrigation water and precipitation samples in the Yellow River irrigation area of the Tumochuan Plain

Location	Type	WIP				SIP			
		Sampling	Time	δD/‰	$\delta^{18}O$/‰	Sampling	Time	δD_{V-SMOW}(‰)	$\delta^{18}O_{V-SMOW}$(‰)
Tianjiagedan	phreatic	DT1	2016-11-10	-77	-9.9	CT1	2017-04-16	-76	-9.8
Wujuniu	phreatic	DW2	2016-11-10	-80	-10.5	CW2	2017-04-16	-77	-10.3
Lixingying	phreatic	DL3	2016-11-11	-67	-8.5	CL3	2017-04-17	-71	-9.2
Xihetou	phreatic	DX4	2016-11-11	-81	-11.2	CX4	2017-04-17	-81	-11.2
Lianhe	phreatic	DL5	2016-11-11	-77	-10	CLH5	2017-04-17	-76	-10
Jinqianpu	phreatic	DJ6	2016-11-12	-74	-9.5	CJ6	2017-04-18	-71	-9.4
Hesenmao	phreatic	DH7	2016-11-12	-81	-10.9	CH7	2017-04-18	-80	-10.9
Houhuangdi	phreatic	DH8	2016-11-13	-81	-11.1	CH8	2017-04-19	-81	-11.1
Saiwusu	phreatic	DS9	2016-11-13	-73	-9.4	CS9	2017-04-19	-73	-9.4
Dongheisha	Phreatic	DD10	2016-11-14	-79	-10.3	CD10	2017-04-20	-78	-10.3
Xinli	phreatic	DX11	2016-11-14	-87	-11.5	CX11	2017-04-20	-87	-11.4
Zhongminsheng	phreatic	DZ12	2016-11-14	-79	-10.8	CZ12	2017-04-20	-78	-10.8
MinShengCanal	irrigation	DH01	2016-11-15	-64	-8.8	CH01	2017-04-21	-62	-8.4
YueJinCanal	irrigation	DH02	2016-11-15	-64	-8.8	CH02	2017-04-21	-62	-8.4
MinZuTuanJieCanal	irrigation	DH03	2016-11-15	-64	-8.8	CH03	2017-04-21	-63	-8.4
Maodai	precipitation	DY00	2016-11-10	-73	-10.9	CY00	2017-04-12	-72	-10.9

As shown in Fig. 7, except the groundwater sampled in Xinli Village in the southeast of the study area (artesian zone), both δD and $\delta^{18}O$ of the groundwater sampled in the WIP and SIP are almost distributed in green, blue, and red elliptic zones. Groundwater samples plot close to right of the meteoric water line of Baotou, which indicates that evaporation occurs in the process of precipitation (Li et al. 2016c; Qian et al. 2013) and the origin of the groundwater is precipitation. The values of stable isotopes (δD and $\delta^{18}O$) of groundwater sampled during both periods are almost identical, which signifies that winter irrigation and spring irrigation exert equivalent impacts on the groundwater. The stable isotopes (δD and $\delta^{18}O$) of groundwater sampled in Lixingying Village are in the lower right of the GMWL (red zone), indicating that irrigation water directly replenishes the groundwater with evaporating in the process of infiltration. The stable isotopes (δD and $\delta^{18}O$) of groundwater sampled in Tianjiagedan Village, Wujuniu Village, Lianhe Village, Jinqianpu Village, Saiwusu Village, and Dongheishatu Village are just below the GMWL (green zone), which are less than those in the red zone. It's possibly because the groundwater in these villages is replenished from not only the runoff formed at high-elevation regions in the north of the study area but also the recharge from local precipitation and irrigation water. The stable isotopes (δD and $\delta^{18}O$) of groundwater sampled in Xiheyan Village, Hesenmao Village, and Houhuangdi Village are in the lower left of the GMWL (blue zone). Therefore, the groundwater in the blue zone is replenished through precipitation and lateral recharge.

Conclusions

(1) The pattern for the mean anions and cations concentrations was, in decreasing order, SO_4^{2-}>Cl^->HCO_3^->NO_3^- and Na^+>Mg^{2+}>Ca^{2+}>K^+, respectively. The average contents of Na^+, SO_4^{2-} and Cl^- are much higher than other ions in groundwater, regardless of reason. The concentrations of main ions of groundwater in the WIP are a little higher than in the SIP, which may be melt snow and ice in spring.

(2) Hydrochemical types and distributions of the groundwater, regardless of reason, were almost identical. There are four hydrochemical types of groundwater, i.e., HCO_3•Cl•SO_4-Na•Ca•Mg, SO_4•Cl-Na, HCO_3•Cl-Na•Mg, and Cl-Na. From northwest to southeast, the hydrochemical type changed from HCO_3•Cl•SO_4-Na•Ca•Mg to SO_4•Cl-Na and finally to Cl-Na. The central area contained a high concentration of SO_4^{2-}, which may be attributed to dissolution of mirabilite.

(3) The main iron contents in groundwater are affected by mineral dissolution besides of evaporation, which are mainly derive from the dissolved rock salt, gypsum, mirabilite, and evaporates. Cation exchange takes place in the aquifers and is likely to play an important role in the evolution of hdrochemistry in the study area.

(4) The values of stable isotopes (δD and $\delta^{18}O$) of groundwater sampled during both periods are almost identical, which signifies that winter irrigation and spring irrigation exert equivalent impacts on the groundwater. Groundwater is directly replenished by irrigation water with evaporating in the process of infiltration around the area of Lixingying Village, and is replenished from not only the runoff formed at high-elevation regions in the north of the study area but also the recharge from local precipitation and irrigation water around the areas of Tianjiagedan Village, Wujuniu Village, Lianhe Village, Jinqianpu Village, Saiwusu Village, and Dongheishatu Village, and is replenished through precipitation and lateral recharge around the areas of Xiheyan Village, Hesenmao Village, and Houhuangdi Village.

Declarations

Acknowledgments

This research was financially supported by the China National Scientific and Technical Support Program (Grant 2018YFC0406402) and the Basic Scientific Research Foundation Special Project of the China Institute of Water Resources and Hydropower Research (nos. MK2020J10) and the National Natural Science Foundation of China (nos. 42072291).

References

1. Adhikary PP, Chandrasekhran H, Dash CJ, Jakhar P (2014) Integrated isotopic and hydrochemical approach to identify and evaluate the source and extend of groundwater pollution in West Delhi, India. Indian Journal of Soil Conservation 42(1): 17-28. https://www.researchgate.net/publication/261991485
2. Rautio A, Niemi KK (2015) Chemical and isotopic tracers indicating groundwater/surface-water interaction within a boreal lake catchment in Finland. Hydrogeology Journal 23(4): 687-705. http:// doi.org//10.1007/s10040-015-1234-5
3. Craig H (1961) Isotopic Variations in Meteoric Waters [J]. Science 133:1702-1703. https://doi.org/10.1126/science.133.3465.1702
4. Chen YM, Gao ZP, Chen ZL, Li W, Wang Q, Ma XM, Guo HM (2019) Distribution characteristics and genesis of strontium-bearing mineral water in Tailai basin. Geology in China 46(6):1-11(**in Chinese**).
5. Farid I, Zouari K, Rigane A, Beji R (2015) Origin of the groundwater salinity and geochemical processes in detrital and carbonate aquifers: Case of Chougafiya basin (Central Tunisia). Journal of Hydrology, 530: 508-532. https://doi.org/10.1016/j.jhydrol.2015.10.009
6. Feng HB, Dong SG, Shi XL, Wang KL, Liu BW, Li ZK, Liu XB (2016) The spatial distribution and its formed mechanism of fluoride in the unconfined and confined groundwater of Tuoketuo County, Inner Mongolia. Geoscience 35(2):139-148 (**in Chinese**).
7. Gao CR, Liu WB, Feng CE, Liu B, Song JX (2014) Distribution characteristics of saline groundwater and high-arsenic groundwater in the Hetao Plain, Inner Mongolia. Acta Geoscientica Sinica 35(2):139-148(**in Chinese**).
8. Gibbs RJ. (1970). Mechanisms Controlling World Water Chemistry [J]. Science, 170(3962): 1088-1090. http://doi.org//10.1126/science.170.3962.1088
9. Gui HR, Chen S (2016) Isotopic geochemical characteristics of groundwater and its geological significance in Sunan mining area. Earth Science Frontiers 23(3):133-139. http://doi.org/10.13745/j.esf.2016.03.017
10. Guo HM, Zhang Y, Xing L, Jia YF (2012) Spatial Variation in Arsenic and Fluoride Concentrations of Shallow Groundwater from the Town of Shahai in the Hetao basin, Inner Mongolia[J]. Applied Geochemistry 27(11): 2187-2196.http://doi.org/10.1016/j.apgeochem.2012.01.016
11. Guo HM, Zhang B, Li Y, Wei L, Zhang Y (2010) Concentrations and patterns of rare earth elements in high arsenic groundwaters from the Hetao Plain, Inner Mongolia. Earth Science Frontiers 17(6):059-066(**in Chinese**).

12. Guo XY, Feng Q, Liu W, Li ZX, Wen XH, Si JH, Xi HY, Guo R, Jia B (2015) Stable isotopic and geochemical identification of groundwater evolution and recharge sources in the arid Shule River Basin of northwestern China. Hydrol Process 29(22): 4703-4718.http://doi.org/10.1002/hyp.10495
13. Han Y, Wang GC, Cravotta CA, Hu WY, Bian YY, Zhang ZW, Liu YY (2013) Hydrogeochemical evolution of Ordovician limestone groundwater in Yanzhou, North China. Hydrol Process 27(16):2247-2257. http://doi.org/10.1002/hyp.9297
14. He S, Li P (2020) A MATLAB based graphical user interface (GUI) for quickly producing widely used hydrogeochemical diagrams. Geochemistry 80(4):125550. https://doi.org/10.1016/j.chemer.2019.125550
15. He S, Wu JH (2019) Hydrogeochemical characteristics, groundwater quality and health risks from hexavalent chromium and nitrate in groundwater of Huanhe Formation in Wuqi County, northwest China. Expo Health 11(2):125-137. http://doi.org/10.1007/s12403-018-0289-7
16. He XD, Wu JH, He S (2019) Hydrochemical characteristics and quality evaluation of groundwater in terms of health risks in Luohe aquifer in Wuqi County of the Chinese Loess Plateau, northwest China. Hum Ecol Risk Assess 25(1-2):32-51. https://doi.org/10.1080/10807039.2018.1531693
17. He X, Ma T, Wang Y X, Deng Y M, Huang B, He J, Zhao J, Tian C Y, Li Z L (2010) Geochemical characteristics of the As-bearing aquifer in the Hetao plain, Inner Mongolia. Geology in China 37(3):781-788(**in Chinese**)
18. Huang QB, Qin XQ, Liu PY, Cheng RR, Li TF (2019) Regional evolution and control factors of karst groundwater in Liulin spring catchment. Environ Sci 40(5):2132-2142. http://kns.cnki.net/kcms/detail/detail.aspx?doi=10.13227/j.hjkx.201811021
19. Li PY (2020a) To make the water safer. Expo Health 12(3):337-342. https://doi.org/10.1007/s12403-020-00370-9
20. Li PY (2020b) Meeting the environmental challenges. Hum Ecol Risk Assess 26(9):2303-2315. https://doi.org/10.1080/10807039.2020.1797472
21. Li PY, Wu JH, Qian H (2013) Assessment of groundwater quality for irrigation purposes and identification of hydrogeochemical evolution mechanisms in Pengyang County, China. Environ Earth Sci 69(7): 2211-2225. http://doi.org/10.1007/s12665-012-2049-5
22. Li PY, Wu JH, Qian H (2016a) Hydrochemical appraisal of groundwater quality for drinking and irrigation purposes and the major influencing factors: a case study in and around Hua County, China. Arab J Geosci 9(1):15. https://doi.org/10.1007/s12517-015-2059-1
23. Li PY, Wu JH, Qian H, Zhang YT, Yang N, Jing LJ, Yu PY (2016b) Hydrogeochemical characterization of groundwater in and around a wastewater irrigated forest in the southeastern edge of the Tengger Desert, northwest China. Expo Health 8(3):331-348. https://doi.org/10.1007/s12403-016-0193-y
24. Li PY, Wu HJ, Qian H (2016c) Preliminary assessment of hydraulic connectivity between river water and shallow groundwater and estimation of their transfer rate during dry season in the Shidi River, China. Environ Earth Sci 75(2):99. https://doi.org/10.1007/s12665-015-4949-7
25. Li PY, Wu JH, Tian R, He S, He XD, Xue CY, Zhang K (2018) Geochemistry, hydraulic connectivity and quality appraisal of multilayered groundwater in the Hongdunzi Coal Mine, northwest China. Mine Water Environ 37(2):222-237. https://doi.org/10.1007/s10230-017-0507-8
26. Li PY, He XD, Li Y, Xiang G (2019a) Occurrence and health implication of fluoride in groundwater of loess aquifer in the Chinese Loess Plateau: A Case Study of Tongchuan, northwest China. Expo Health 11:95–107. http://doi.org/10.1007/s12403-018-0278-x.
27. Li ZJ, Yang QC, Yang YS, Ma HY, Wang H, Luo JN, Bian JM, Martin JD (2019b) Isotopic and geochemical interpretation of groundwater under the influences of anthropogenic activities. Journal of Hydrology 576: 685-597.http://doi.org/10.1016/j.jhydrol.2019.06.037.
28. Liu XB, Dong SG, Liu BW, Feng HB, Li ZK, Liu LW (2017) Hydrogeoehemical Characteristics and Genesis of Groundwater in the Tumochuan Plain of Inner Mongolia. Acta Geoscientica Sinica 38(6):919-929. https://doi.org/10.3975/cagsb.2017.06.07
29. Ma B, Jin MG, Liang X, Li J (2018) Groundwater mixing and mineralization processes in a mountain-oasis-desert basin□northwest China: hydrogeochemistry and environmental tracer indicators□ Hydrogeology Journal□26(1) : 233-250□https://doi.org/10.1007/s10040-017-1659-0
30. Marandi A, Shand P (2018) Groundwater chemistry and the Gibbs Diagram. Applied Geochemistry 97: 209-212□ https://doi.org/10.1016/j.apgeochem.2018.07.009
31. Piper A (1944) A graphic procedure in the geochemical interpretation of water-analyses. Eos Transactions American Geophysical Union 25(6):914-928. https://doi.org/10.1029/TR025i006p00914
32. Qi HH, Ma CM, He ZK, Hu XJ, Gao L (2019) Lithium and its isotopes as tracers of groundwater salinization: A study in the southern coastal plain of Laizhou Bay□China. Science of the total Environment 650: 878-890. https://doi.org/10.1016/j.scitotenv.2018.09.122
33. Qian H, Li PY, Wu JH, Zhou YH (2013) Isotopic characteristics of precipitation, surface and ground waters in the Yinchuan Plain, northwest China. Environ Earth Sci 70(1):57-70. https://doi.org/10.1007/s12665-012-2103-3

34. Qian H, Wu JH, Zhou YH, Li PY (2014) Stable oxygen and hydrogen isotopes as indicators of lake water recharge and evaporation in the lakes of the Yinchuan Plain. Hydrol Process 28:3554–3562. https://doi.org/10.1002/hyp.9915
35. Redwan M, Abdel Moneim AA (2016) Factors controlling groundwater hydrogeochemistry in the area west of Tahta，Sohag，Upper Egypt， Journal of African Earth Science 118: 328-338. https://doi.org/10.1016/j.jafrearsci.2015.10.002
36. Ren XF, Li PY, He XD, Su FM, Elumalai V (2021) Hydrogeochemical processes affecting groundwater chemistry in the central part of the Guanzhong Basin, China. Arc Environ Contam Toxicol 80(1):74-91. https://doi.org/10.1007/s00244-020-00772-5
37. Scanlon BR, Keese KE, Flint AL, Flint LE, Gaye CB, Edmunds WM, Simmers I (2006) Global synthesis of groundwater recharge in semiarid and arid regions. Hydrol Process 20(15): 3335-3370.https://doi.org/10.1002/hyp.6335
38. Schoeller, H (1977) Geochemistry of Groundwater. In: Brown, R.H., Konoplyantsev, A.A., Ineson, J. and Kovalevsky, V.S., Eds., Groundwater Studies: An International Guide for Research and Practice, UNESCO, Paris, 1-18.
39. Shen ZL, Zhu WH, Zhong ZS (1993) Hydrogeochemistry basis. Geological Publishing House, Beijing **(in Chinese)**
40. Su ZM, Wu JH, He XD, Elumalai V (2020) Temporal changes of groundwater quality within the groundwater depression cone and prediction of confined groundwater salinity using Grey Markov model in Yinchuan area of northwest China. Expo Health 12(3):447-468. https://doi.org/10.1007/s12403-020-00355-8
41. Sun HY, Mao QG, Wei XF, Zhang HQ, Xi YZ. (2018) Hydrogeochemical characteristics and formation evolutionary mechanism of the groundwater system in the Hami basin. Geology in China, 45(6):1128-1141 **(in Chinese)**
42. Wang JZ, Wu JL, Zeng HA, Bai RD (2013) Characteristics of water isotope and hydrochemistry in Hetao Plain of Inner Mongolia. Journal of Earth Sciences and Environment 35(4):104-112. https://doi.org/10.3969/j.issn.1672-6561.2013.04.012
43. Wang XX, Wang WK, Wang ZF, Zhao JL, Xie HL, Wang XD (2014) Hydrochemical characteristics and formation mechanism of river water and groundwater along the downstream Luanhe River, northeastern China. Hydrogeology & Engineering Geology 41(1): 25-33, 73**(in Chinese).**
44. Wang LH，Dong YH，Xu ZF，Qiao XJ (2017a) Hydrochemical and isotopic characteristics of groundwater in the northeastern Tennger Desert，northern China. Hydrogeology Journal 25(8):2363-2375. https://doi.org/10.1007/s10040-017-1620-2
45. Wang ZH, Liu W, Zhao YP, Zhang ZF, Du XF (2017b) Hydrochemical evolution laws of groundwater in typical irrigation district of the Yellow River. Yellow River 39(supplement1):63-65**(in Chinese)**.
46. Wu JH, Li PY, Qian H, Duan Z, Zhang XD (2014) Using correlation and multivariate statistical analysis to identify hydrogeochemical processes affecting the major ion chemistry of waters: Case study in Laoheba phosphorite mine in Sichuan, China. Arab J Geosci 7(10):3973-3982. https://doi.org/10.1007/s12517-013-1057-4
47. Wu JH, Li PY, Qian H (2015) Hydrochemical characterization of drinking groundwater with special reference to fluoride in an arid area of China and the control of aquifer leakage on its concentrations. Environ Earth Sci 73(12):8575-8588. https://doi.org/10.1007/s12665-015-4018-2
48. Wu JH, Zhang YX, Zhou H (2020) Groundwater chemistry and groundwater quality index incorporating health risk weighting in Dingbian County, Ordos basin of northwest China. Geochemistry 80(4):125607. https://doi.org/10.1016/j.chemer.2020.125607
49. Xiao J, Jin Z D, Zhang F, Wang J(2012)Solute geochemistry and its sources of the groundwaters in the Qinghai Lake catchment, NW China. Journal of Asian Earth Sciences 52: 21-30，https://doi.org/10.1016/j.jseaes.2012.02.006
50. Xiao J, Jin ZD, Wang J, Zhang F. (2015) Hydrochemical characteristics, controlling factors and solute sources of groundwater within the Tarim River Basin in the extreme arid region, NW Tibetan Plateau. Quaternary International 380-381: 237-246， https://doi.org/10.1016/j.quaint.2015.01.021
51. Zhao Y, Wang CL, Xiang W, Zhang SJ (2019) Evaluation of the hydrochemical evolution characteristics and renewable capacity of deep fresh groundwater in the Hangzhou Bay New Zone, China. Environ Earth Sci 78(22): 644-658.https://doi.org/10.1007/s12665-019-8645-x
52. Zhang T, Cai WT, Li YZ, Zhang ZY, Geng TT, Biao C, Zhao M, Cai YM (2017) Major ionic features and their possible controls in the water of the Niyang River basin. Environmental Science 38(11) : 4537-4545，https://doi.org/10.13227/j.hjkx.201704051
53. Zhang T, He J, Li JJ, Cao YT, Gong L, Liu JW, Bian C, Cai YM (2018) Major ionic features and possible controls in the groundwater in the Hamatong River Basin. Environmental Science 39(11) : 4981-4990，https://doi.org/10.13227/j.hjkx.201804070
54. Zhang YT, Wu JH, Xu B (2018) Human health risk assessment of groundwater nitrogen pollution in Jinghui canal irrigation area of the loess region, northwest China. Environ Earth Sci 77(7):273. https://doi.org/10.1007/s12665-018-7456-9

Figures

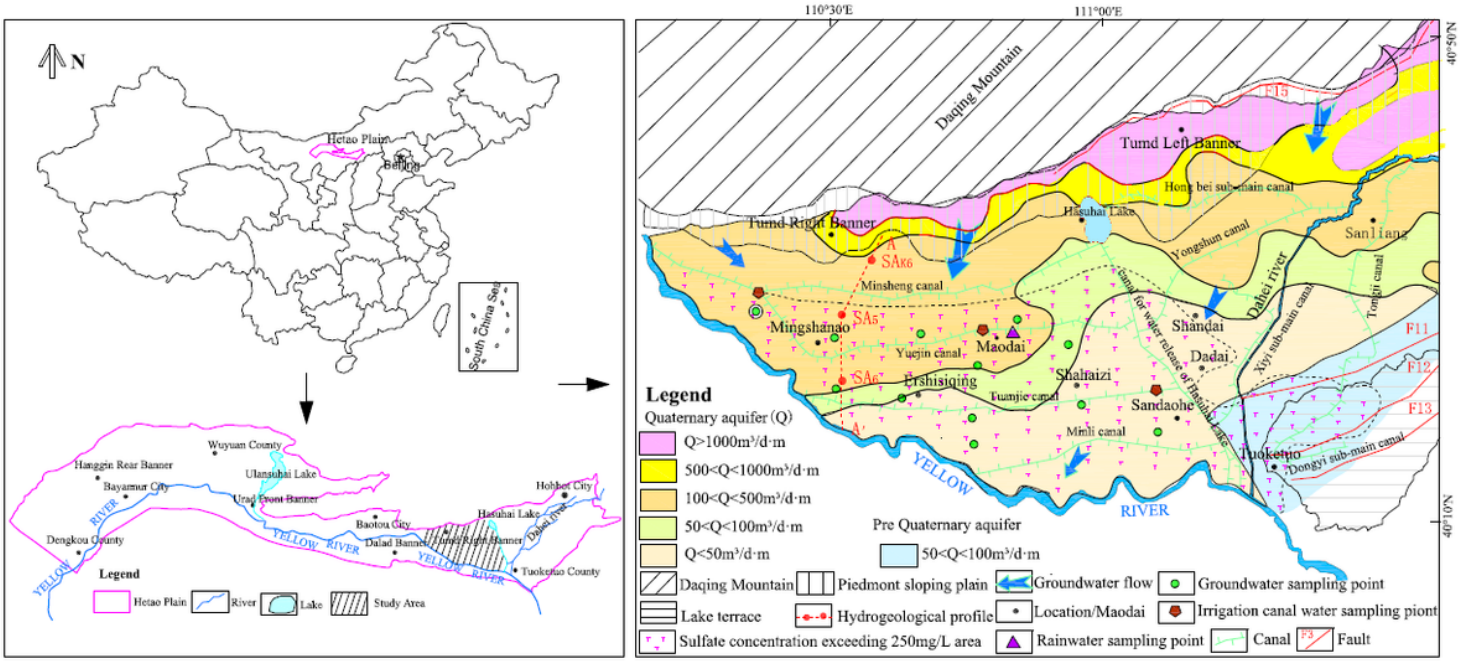

Figure 1

Location of study area, hydrogeological map, and sampling sites

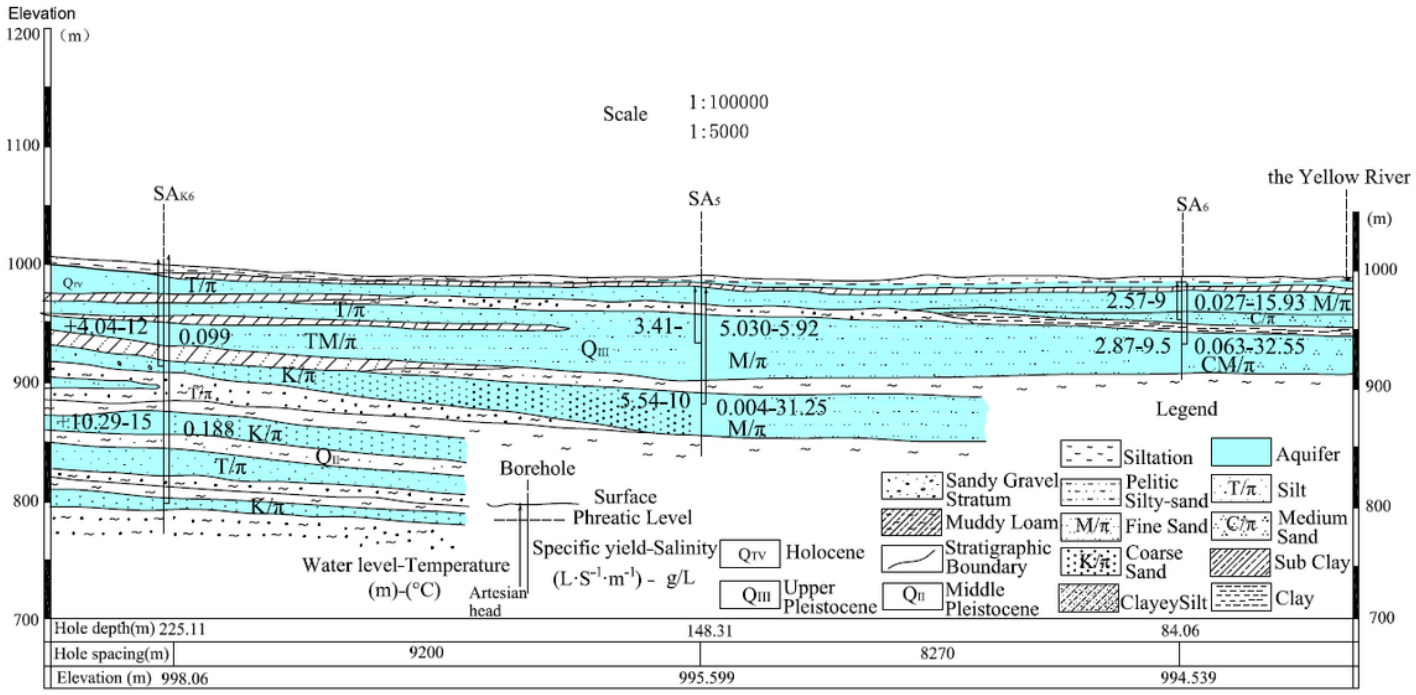

Figure 2

Hydrogeological section（A-A'）

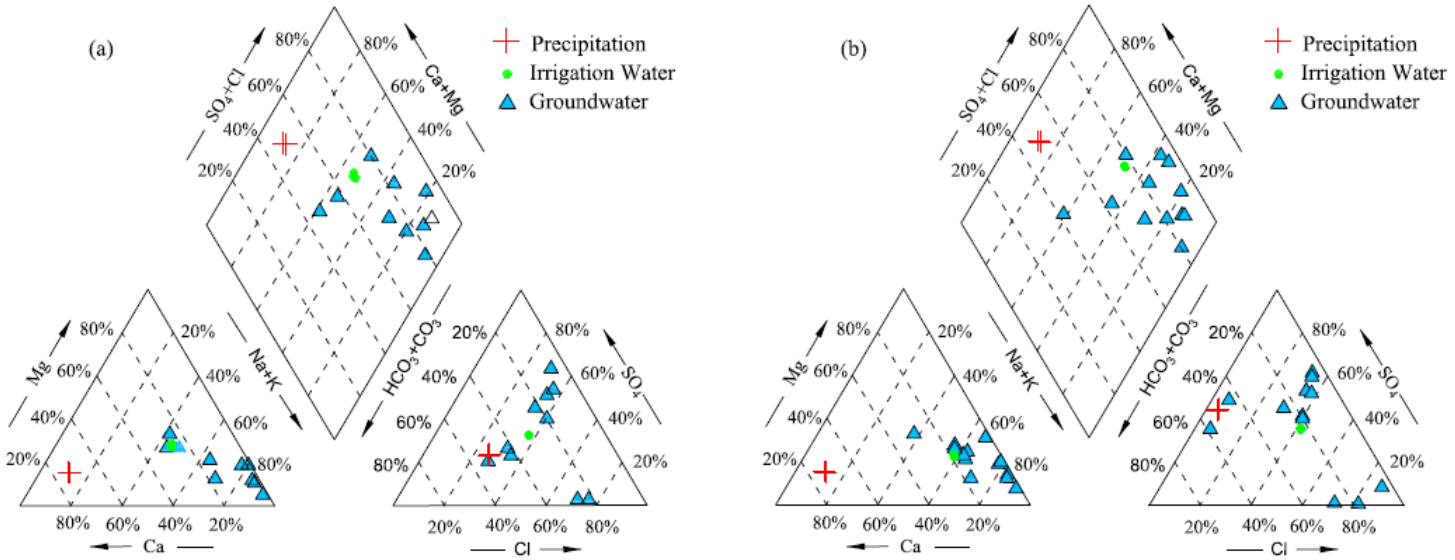

Figure 3

Piper diagram of groundwater、irrigation water and precipitation: (a) WIP, November 2016; (b) SIP, April 2017

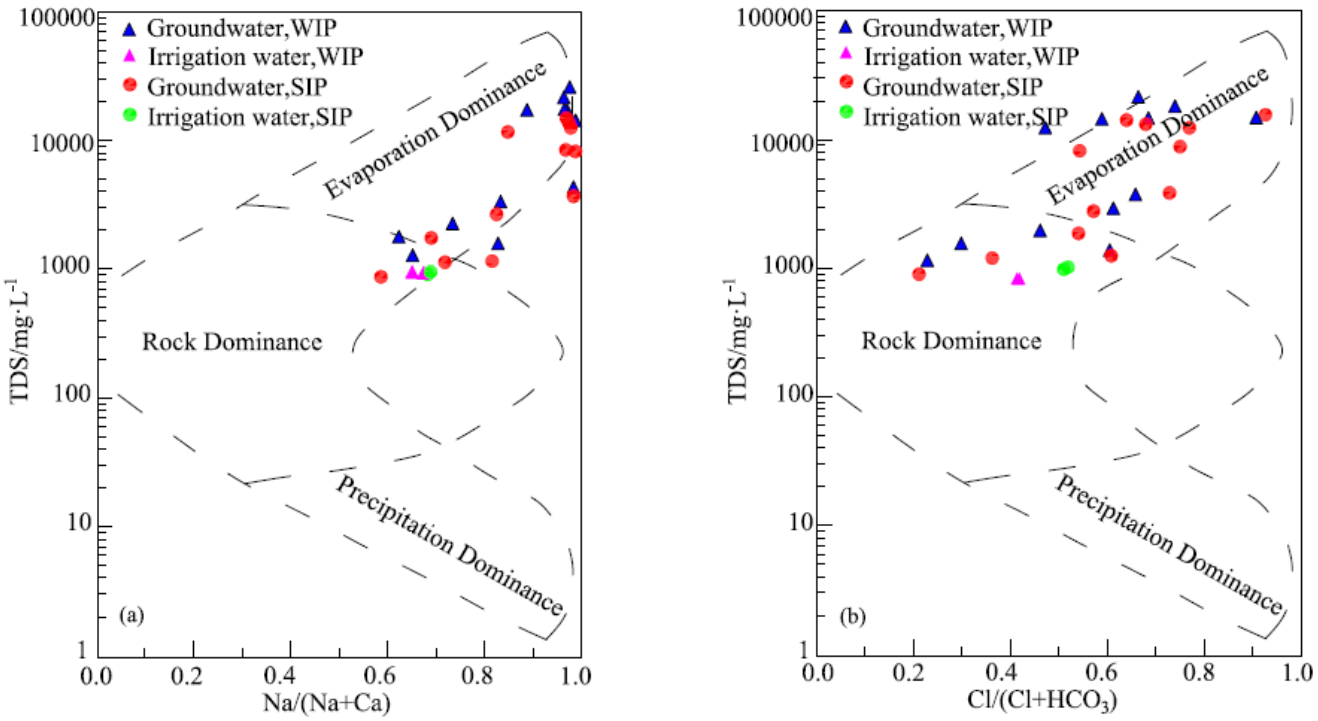

Figure 4

Gibbs diagram of groundwater and irrigation water

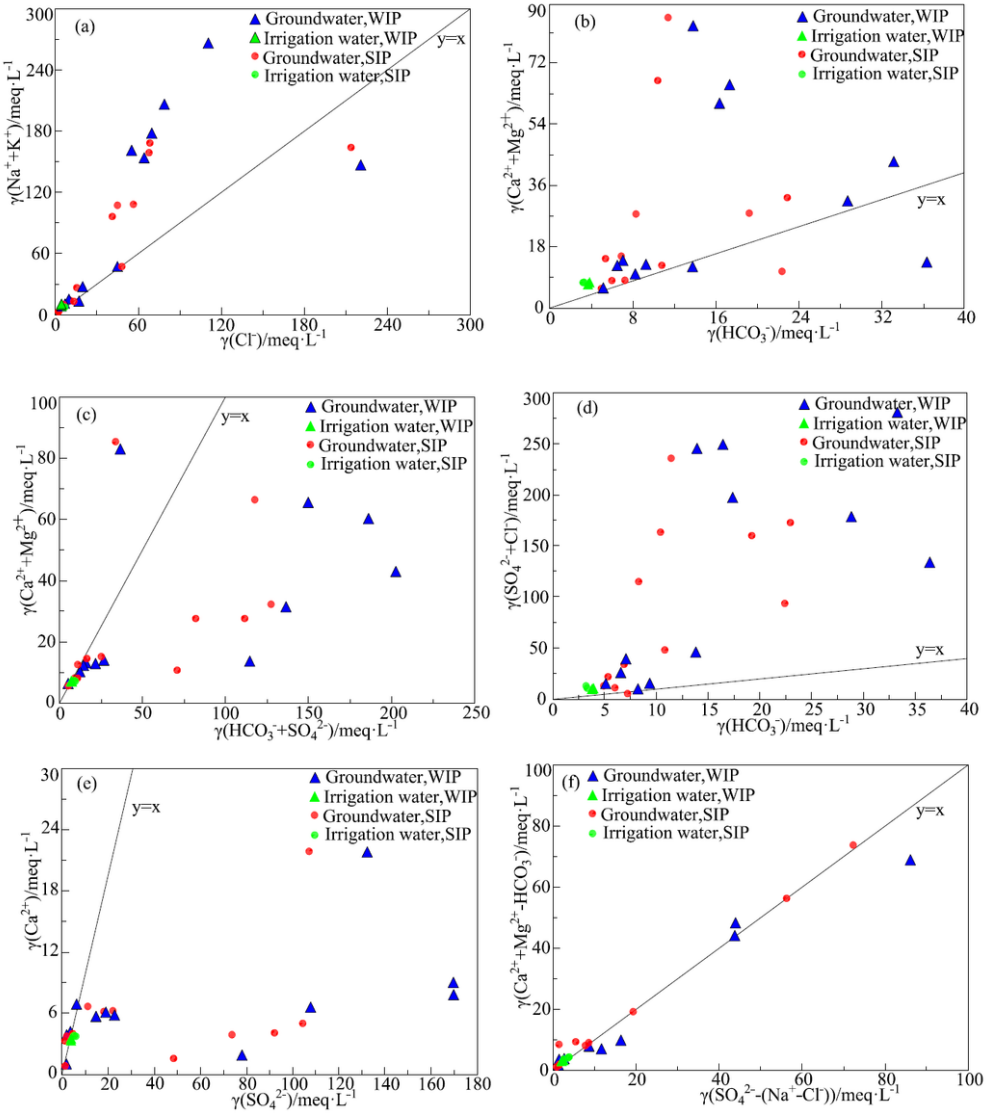

Figure 5

Ionic relationships of groundwater in the study area

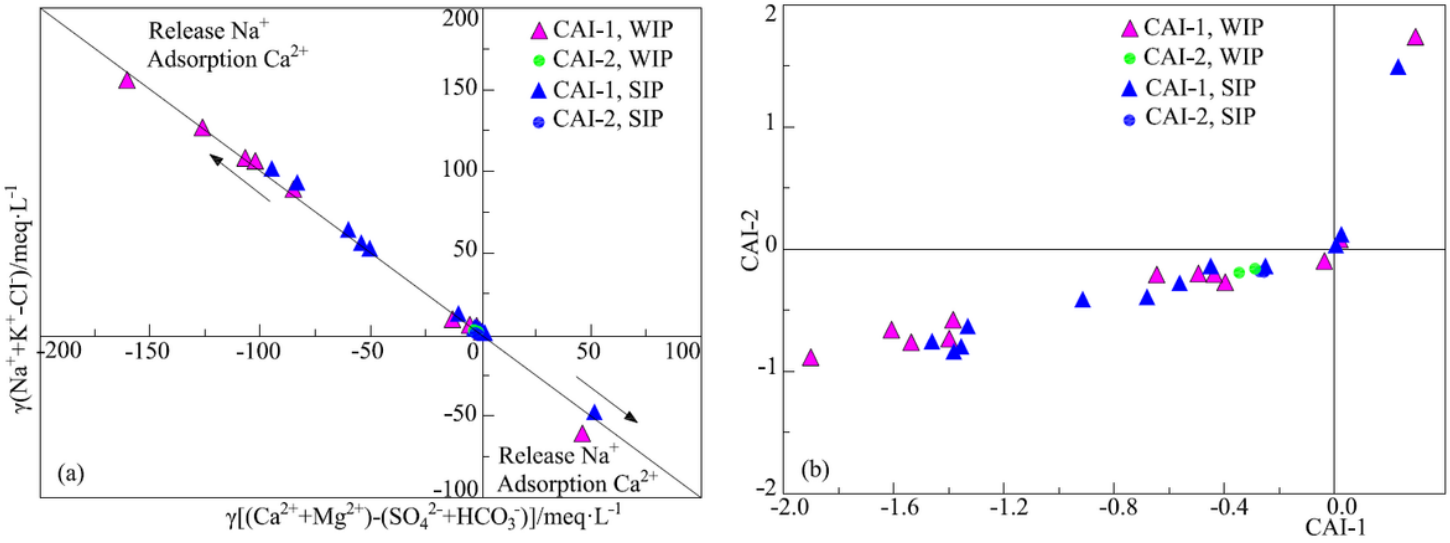

Figure 6

Diagram of ion exchange: (a) (Mg2++Ca2+-SO42-HCO3-) vs. (Na++K+-Cl-); (b) choro-alkaline indices vs. TDS

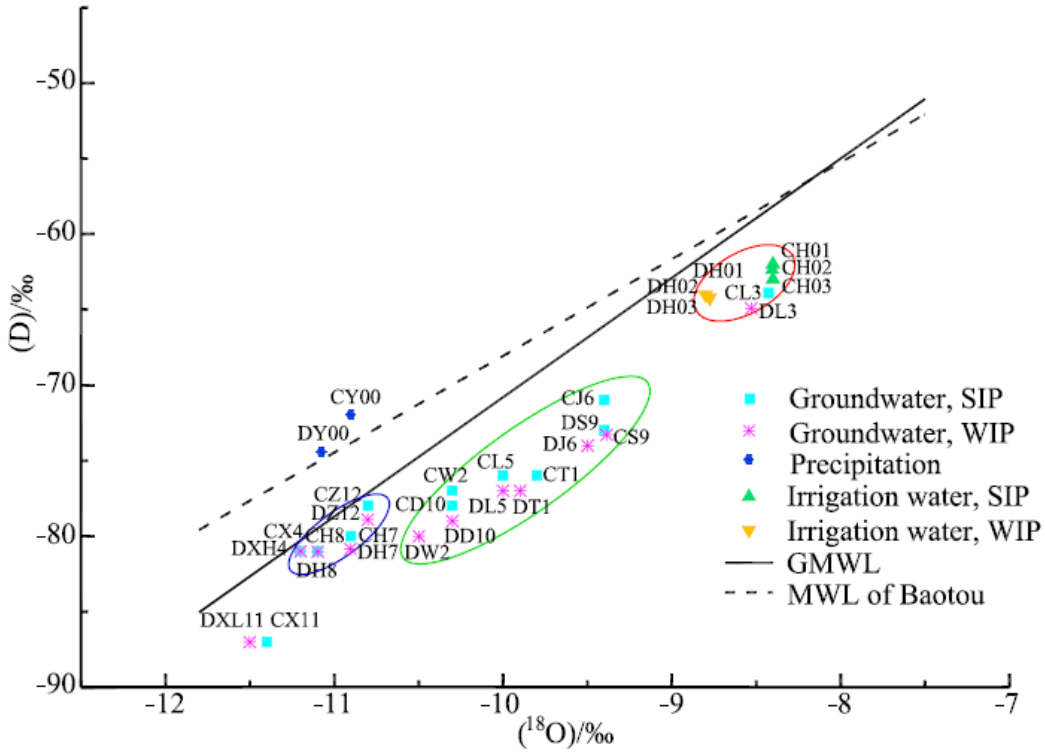

Figure 7

Relationship of oxygen and hydrogen stable isotope in precipitation, irrigation water and groundwater